THE JOURNAL OF PHYSICAL CHEMISTRY A
A JOURNAL OF THE AMERICAN CHEMICAL SOCIETY

pubs.acs.org/JPCA

Article

Amino Acids Compete with Ammonia in Sulfuric Acid-Based Atmospheric Aerosol Prenucleation: The Case of Glycine and Serine

Conor J. Bready, Sara Vanovac, Tuguldur T. Odbadrakh, and George C. Shields*

Cite This: *J. Phys. Chem. A* 2022, 126, 5195−5206

Read Online

ACCESS | Metrics & More | Article Recommendations | Supporting Information

ABSTRACT: We present a computational investigation of the sulfuric acid, glycine, serine, ammonia, and water system to understand if this system can form prenucleation clusters, which are precursors to larger aerosols in the atmosphere. We have performed a comprehensive configurational search of all possible clusters in this system, starting with the four different monomers and zero to five waters. Accurate Gibbs free energies of formation have been calculated with the DLPNO-CCSD(T)/complete basis set (CBS) method on ωb97xd/6-31++G** geometries. For the dry dimers of sulfuric acid, the weakest base, serine, is found to form the most stable complex, which is a consequence of the strong di-ionic complex formed between the bisulfate ion and the protonated serine cation. For the dry dimers without sulfuric acid, the glycine−serine complex is more stable than the glycine−ammonia or serine−ammonia complexes, stemming from the detailed structure and not related to base strength. For the larger complexes, sulfuric acid deprotonates and the proton is shifted to glycine, serine, or ammonia. The two amino acids and ammonia are almost interchangeable and there is no easy way to predict which molecule will be protonated without the calculated results. Assuming reasonable starting concentrations and a closed system of sulfuric acid, glycine, serine, ammonia, and five waters, we predict the concentrations of all possible complexes at two temperatures spanning the troposphere. The most negative ΔG° values are a function of the detailed molecular interactions of these clusters. These details are more important than the base strength of ammonia, glycine, and serine.

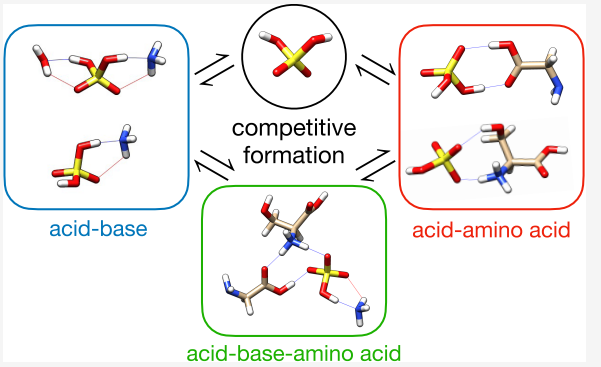

INTRODUCTION

Gas-phase acid−base chemistry plays an important role in the formation and growth of prenucleation clusters in atmospheric new particle formation (NPF).[1,2] By acting as cloud condensation nuclei (CCN), these clusters can affect the atmosphere's ability to absorb or reflect radiation by modulating the formation and lifetime of clouds. This is particularly important in climate change as clouds have the potential to cool the atmosphere by scattering incoming solar radiation.[3] New particle formation starts with small gas-phase molecular clusters of 1−3 nm in diameter whose thermodynamic stability is determined through favorable intermolecular interactions. As an abundant component of the atmosphere, sulfuric acid is a fundamental nucleator that forms stable clusters with water,[4−6] various atmospheric bases,[7,8] and organic molecules.[9,10] The stability and growth of sulfuric acid clusters have been studied extensively using both experimental and theoretical methods.[11−13] State-of-the-art experimental techniques are just now accessing the sub-3 nm size regime, but still have difficulty interpreting the effects of humidity due to the low-pressure environment necessary for size resolution.[14] Due to this absence of water in experimental data, computational efforts have mainly focused on the stability and growth of dry prenucleation clusters.[12]

Computational studies of sulfuric acid-based atmospheric prenucleation clusters have shown that acid−base clusters are particularly stable. Sulfuric acid can form dimers with atmospheric bases whose stability is thought to follow the gas-phase basicity trend of the constituent bases.[7,15−24] However, a recent shift in attention toward other atmospheric trace constituents has revealed that gas-phase acidity and basicity can take a secondary role to structural features of the prenucleation cluster, such as hydrogen-bond topology and intermolecular interactions. In small, dry clusters, electrostatics often follows the gas-phase basicity trend,[25,26] while intermolecular forces can play a dominant role due to functional groups on bases.[27,28] The binding energy of small sulfuric acid−ammonia−amine clusters is primarily determined by gas-phase basicity, while larger clusters follow aqueous basicity.[29] As clusters consist of a larger number of different

Received: May 22, 2022
Revised: July 18, 2022
Published: July 27, 2022

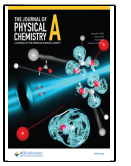

https://doi.org/10.1021/acs.jpca.2c03539
J. Phys. Chem. A 2022, 126, 5195−5206

species, hydrogen-bond topology becomes more important than acid−base strength. This was demonstrated by our recent work where we found that formic acid is as effective as ammonia for the formation of clusters with sulfuric acid and water.[30] Including water molecules results in the formation of hydrogen-bond networks.[28,31] Sulfuric acid can form comparably stable clusters with atmospheric species other than bases,[9] such as formic acid[10,30] and amino acids.[32−35] In these cases, the ability of functional groups to form strong intermolecular interactions is key to the thermodynamic stability of the cluster.[36,37] Amino acids are enriched in sea spray aerosols by up to 7 orders of magnitude,[38] and they are driven to the aerosol air−water interface in salts and acidic environments.[39] At the interface, they are more reactive, including for the formation of peptide bonds.[40−43] Yet, amino acids without the presence of sulfuric acid do not drive aerosol formation.[44] Given these recent advances, we have undertaken a systematic study of the thermodynamic stability of sulfuric acid prenucleation clusters in the presence of ammonia, simple amino acids, and water to further investigate the role of intermolecular forces and hydrogen-bond topology in atmospheric new particle formation.

We present our computational investigation of the (SA)-(Gly)(Ser)(A)(W)0-5 system, where SA = sulfuric acid, Gly = glycine, Ser = serine, A = ammonia, and W = water. Our methodology is largely based on our previous works,[30,44−46] with the exception that we have switched our geometry optimization to the ωb97xD functional and we have compared harmonic, scaled harmonic, and quasi-harmonic corrections to partially correct for anharmonicity for four of the smaller clusters. Then, we describe our results for the geometries and CCSD(T) corrected Gibbs free energies, followed by an analysis of atmospheric implications of these results.

METHODOLOGY

Initial guess geometries of Gly and Ser were generated using the CREST[47] conformational sampling routine on the GFn2[48,49] potential energy surface (PES) using Grimme's XTB program.[49,50] Since symmetry numbers enter the thermodynamic correction expressions,[51] we ensured that our monomer structures contained proper symmetries, which are: SA = C2, A = C3v, and W = C2v. Initial cluster guess geometries were generated using an evolutionary algorithm on the PM7[52,53] PES using the OGOLEM[54,55] configurational sampling program. They were then subject to further refinement and vibrational frequency calculations at the ωb97xD[56,57]/6-31++G**[58−62] level of theory using the Gaussian 16 Rev. B01 program.[63] Further electronic energy corrections were computed at the complete basis set limit (CBS) on the domain local pair natural orbital coupled-cluster PES with single, double, and perturbative triple excitations (DLPNO-CCSD(T))[64−73] and Dunning's cc-pVnZ[74−76] (n = D, T, Q) basis sets using the ORCA 5.0.1 program.[77,78] The three DLPNO-CCSD(T) electronic energies were used in a 4−5 inverse polynomial CBS extrapolation scheme[79] and combined with ωb97xD vibrational frequencies to calculate the thermodynamic corrections H°, S°, and G° at a standard state of 1 atm pressure and temperatures of 216.65, 273.15, and 298.15 K using the THERMO.pl script from the National Institute of Science and Technology.[80] Finally, the equilibrium concentrations of all possible combinations of the monomers were computed using the DLPNO-CCSD(T)/CBS//ωb97xD/6-31++G** energies.[30,44] A diagrammatic representation of our methodology for finding the Gibbs free energy minimum-energy structures is shown in Figure 1.

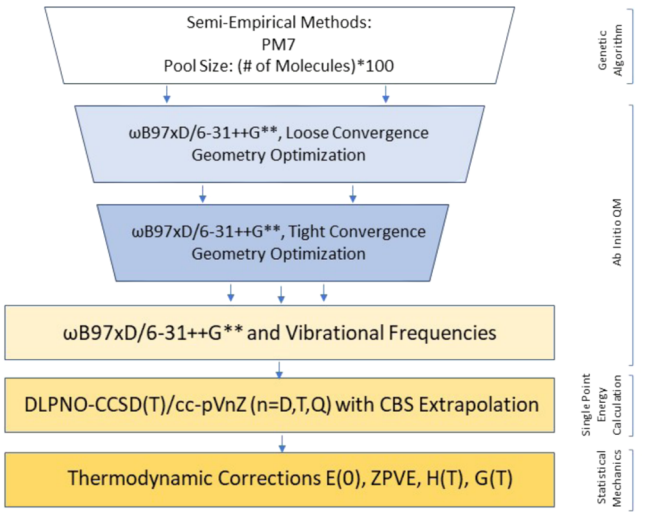

Figure 1. Computational methodology used for this study.

Vibrational Anharmonicity. Comparison of calculated harmonic vibrational frequencies with observed frequencies requires an empirical correction to account for the vibrational anharmonicity.[81] Low-frequency modes are more anharmonic than high-frequency modes, and they can couple with each other as well as with rotational degrees of freedom. Since low-frequency modes contribute the most to the thermal correction to enthalpy and entropy of a system, small deviations in these modes can lead to large errors in Gibbs free energies. Thus, hydrogen-bonded clusters are a real concern for practitioners in the field, who are often reluctant of using calculated harmonic frequencies to estimate free energies at higher temperatures for these weakly bound clusters.[82,83] The most common method to calculate anharmonicity is Barone's second-order vibrational perturbation theory (VPT2),[84,85] where anharmonic corrections are calculated from higher-order derivatives of the potential energy surface; the cubic and semidiagonal quartic force constants are calculated by finite differentiation of the Hessian along the normal mode coordinates. The main drawback of VPT2 is the problem of near-degeneracies, or resonances, as in other perturbation theory methods. To reduce numerical errors in anharmonic frequency calculations, tight convergence criteria need to be enforced for geometry optimization and the Hessian calculations. In addition, as third and fourth derivatives are determined by finite differentiation of analytic Hessians for nuclear displacements along each normal mode, the default 0.250 Å step size[85] often yields erratic anharmonic frequencies for larger molecular clusters, even when both the geometries and energies are tightly converged.[83]

Work on the water dimer and larger water clusters has shed some light on the validity of using scaling or anharmonic calculations to better represent the frequencies of hydrogen-bonded systems.[86−91] The water dimer is the only water cluster system whose vibrational spectrum is fully resolved. Scaling the water dimer HF/6-31G* harmonic frequencies by 0.8928 results in good agreement, with a root-mean-square deviation (RMSD) of 24 cm^{-1} from experiment.[88,92] Combining scaled harmonic frequencies for the intramolecular modes with

https://doi.org/10.1021/acs.jpca.2c03539
J. Phys. Chem. A 2022, 126, 5195−5206

anharmonic frequencies for the intermolecular modes reduces the RMSD to 20 cm^{-1}.

Larger water clusters up to the size of the nonamer have been extensively studied using the frozen-core resolution-of-the-identity MP2 (RI-MP2) method to understand the impact of scaling versus calculating VPT2 anharmonic frequencies.[83] Water clusters can be separated into three distinct regions: intermolecular modes below 1100 cm^{-1}, bending modes between 1100 and 1800 cm^{-1}, and stretching modes that lie above 3000 cm^{-1}. The frequencies in these three different regions were scaled by three different scaling factors and compared with anharmonic results.[83,93] The step size that yielded reasonable anharmonic frequencies for $(H_2O)_n$ = 2−6, 8, 9 was 0.0050 Å. While VPT2 or a three-split scaling scheme yields the most accurate results, a single scaling factor that scales all of the modes to better represent the intermolecular modes also leads to relatively good agreement because the bending and stretching modes are less anharmonic.[83,94,95]

There has been less work published on the scaling of atmospheric clusters consisting of acids and bases. Torrent-Succarrat and co-workers calculated B3LYP anharmonic frequencies for hydrogen-bonded complexes formed from the hydroxyperoxyl radical and formic, acetic, nitric, and sulfuric acids and reported good agreement with experiment.[96] Kurten and co-workers have calculated anharmonic vibrational modes for $H_2SO_4(H_2O)_n$ = 1−4 and $HSO_4^-(H_2O)_n$ = 1−4 clusters.[97] Temelso et al. have applied the same methodology used for water clusters to sulfuric acid hydration using RI-MP2 extrapolated to the complete basis set (CBS) limit.[5] The $\Delta G°$ for the formation of the $H_2SO_4(H_2O)$ dimer and $H_2SO_4(H_2O)_2$ trimer have been obtained experimentally for these two clusters at 298 K and are −3.6 ± 1 and −5.9 ± 1.3 kcal mol^{-1}.[98] The calculated unscaled harmonic, scaled harmonic, and VPT2 anharmonic $\Delta G°$ (298 K) values for the dimer are −2.4, −2.9, and −2.8 kcal mol^{-1}, while for the trimer, they are −3.3, −4.1, and −4.2 kcal mol^{-1}. All of these values are close to the experimental uncertainty, and the scaled harmonic and anharmonic values are within 0.1 kcal mol^{-1} of each other. In an RI-MP2/CBS study of $(H_2SO_4)_2(H_2O)_n$ = 0−6, the scaled harmonic frequencies for the four lowest Gibbs free energy $(H_2SO_4)_2$ clusters at 298 K were all within 0.4 kcal mol^{-1} of the anharmonic values, and similarly for the four lowest $\Delta G°$ (298 K) $(H_2SO_4)(H_2O)$ clusters, the scaled harmonic frequencies were within 0.6 kcal mol^{-1} of the anharmonic values.[6] The mean absolute error (MAE) of the harmonic frequencies relative to the eight anharmonic frequencies was 0.89 kcal mol^{-1}, while the MAE for the scaled harmonic frequencies was 0.25 kcal mol^{-1}.

Due to the importance of vibrational anharmonicities arising from intermolecular interactions, we have examined the effects of using various Gibbs free energy correction schemes to determine the best choice going forward. For $(Gly)(W)_n$ = 1−4, Table 1 displays the Gibbs free energies of hydration computed using (1) harmonic frequencies in the rigid-rotor harmonic-oscillator model (RRHO),[80,99] (2) harmonic frequencies in the rigid-rotor quasi-harmonic-oscillator model (RRQH),[100−102] and (3) scaled harmonic frequencies using Truhlar's ωb97xD ZPE scaling factor of 0.971 for thermochemical calculations from ref 103. Our anharmonic frequencies from second-order vibrational perturbation theory (VPT2)[84,85] suffered from extensive resonances and yielded inaccurate values and are not reported. We note that the calculation of the Gibbs free energy corrections is based on the rigid-rotor harmonic-oscillator partition function and the difference between the methods presented is the manner in which the frequencies enter the partition function. Both the scaled RRHO and VPT2 methods simply replace the RRHO frequencies with new values, while the RRQH method removes low-frequency contributions by incorporating them into the rotational contribution.

Table 1. DLPNO-CCSD(T)/CBS//ωb97xD/6-31++G Gibbs Free Energy Changes Associated with the Hydration of Glycine at a Temperature of 298.15 K and Standard Pressure of 1 atm**

cluster	RRHO	RRQH	scaled RRHO
Gly + W ⇌ (Gly)(W)	1.197	1.443	1.076
Gly + 2W ⇌ $(Gly)(W)_2$	1.804	2.477	1.560
Gly + 3W ⇌ $(Gly)(W)_3$	3.418	5.111	3.056
Gly + 4W ⇌ $(Gly)(W)_4$	6.675	8.398	6.184

Table 1 shows that the RRQH method yields Gibbs free energy changes that are higher than the RRHO values. Using scaled RRHO energies systematically lowers the unscaled RRHO values, while the RRQH values are more positive than the unscaled RRHO energies; therefore, we chose to use scaled RRHO Gibbs free energy corrections for the rest of our work. We note that the SA and Ser clusters are not well behaved in the VPT2 formulation of anharmonic frequency calculations, yielding Gibbs free energies, which are higher than the RRHO values. This could be due to strong anharmonicities that are outside the radius of convergence of second-order perturbation theory. One possible fix for this is to use the vibrational self-consistent field[104,105] (VSCF) method followed by post-SCF corrections such as second-order perturbation theory[106] (VSCF-PT2) or configuration interaction[107] (VSCF-CI); however, the computational cost of acquiring the VSCF wavefunction and higher-order derivatives of the PES are prohibitive for all but small systems.

RESULTS AND DISCUSSION

Formation and Hydration of Sulfuric Acid-Containing Dimers. Table 2 lists the Gibbs free energy changes associated with the formation of sulfuric acid-containing dimers and their subsequent solvation with up to five water molecules, with the corresponding geometries shown in Figure 2. These data allow for the examination of the effects of replacing ammonia with glycine or serine in the sulfuric acid−ammonia dimer. We have defined hydrogen bonds as H---O or H---N distances less than 2.2 Å and with hydrogen-bond angles between 140 and 180°, and have indicated these hydrogen bonds with blue lines in the figures. Close van der Waals contacts, with bond angles less than 140° or bond lengths between 2.2 and 2.4 Å, are indicated by red lines. In the absence of water, the (SA)(Ser) dimer is the most stable structure, which can be attributed to a proton transfer from sulfuric acid to serine's amine group that is stabilized by a strong hydrogen bond from the serine methoxy group to the sulfuric acid molecule. Comparing the (SA)(Ser) hydrogen-bond network to those of (SA)(Gly)(W) and $(SA)(A)(W)_2$ reveals that the transfer of a proton from SA to any amine group only occurs when the SA accepts a strong hydrogen bond from a third entity, i.e., an additional water molecule. This proton transfer is observed to account for about 2 kcal mol^{-1} of stabilization energy. This trend continues in the trimer clusters, as will be discussed later.

https://doi.org/10.1021/acs.jpca.2c03539
J. Phys. Chem. A 2022, 126, 5195−5206

Table 2. DLPNO-CCSD(T)/CBS//ωb97xD/6-31++G Gibbs Free Energy Changes Associated with the Formation and Sequential Hydration of Sulfuric Acid−Glycine, Sulfuric Acid−Serine, and Sulfuric Acid−Ammonia Dimers at Atmospherically Relevant Temperatures and 1 atm Pressure**

cluster	216.65 K	273.15 K	298.15 K
SA + Gly ⇌ (SA)(Gly)	−8.81	−6.79	−5.90
(SA)(Gly) + W ⇌ (SA)(Gly)(W)	−5.18	−3.43	−2.65
$(SA)(Gly)(W) + W \rightleftharpoons (SA)(Gly)(W)_2$	−3.55	−1.55	−0.67
$(SA)(Gly)(W)_2 + W \rightleftharpoons (SA)(Gly)(W)_3$	−2.14	−0.46	0.17
$(SA)(Gly)(W)_3 + W \rightleftharpoons (SA)(Gly)(W)_4$	−1.53	0.49	1.44
$(SA)(Gly)(W)_4 + W \rightleftharpoons (SA)(Gly)(W)_5$	−1.95	−0.40	0.32
SA + Ser ⇌ (SA)(Ser)	−12.26	−10.20	−9.28
(SA)(Ser) + W ⇌ (SA)(Ser)(W)	−4.94	−2.99	−2.12
$(SA)(Ser)(W) + W \rightleftharpoons (SA)(Ser)(W)_2$	−3.72	−1.88	−1.06
$(SA)(Ser)(W)_2 + W \rightleftharpoons (SA)(Ser)(W)_3$	−2.25	−0.69	−0.01
$(SA)(Ser)(W)_3 + W \rightleftharpoons (SA)(Ser)(W)_4$	−1.34	0.82	1.78
$(SA)(Ser)(W)_4 + W \rightleftharpoons (SA)(Ser)(W)_5$	1.22	2.86	3.58
SA + A ⇌ (SA)(A)	−8.66	−7.10	−6.41
(SA)(A) + W ⇌ (SA)(A)(W)	−3.35	−1.48	−0.65
$(SA)(A)(W) + W \rightleftharpoons (SA)(A)(W)_2$	−6.61	−4.73	−3.91
$(SA)(A)(W)_2 + W \rightleftharpoons (SA)(A)(W)_3$	−1.15	0.41	1.10
$(SA)(A)(W)_3 + W \rightleftharpoons (SA)(A)(W)_4$	−3.11	−1.09	−0.20
$(SA)(A)(W)_4 + W \rightleftharpoons (SA)(A)(W)_5$	−0.65	1.56	2.54

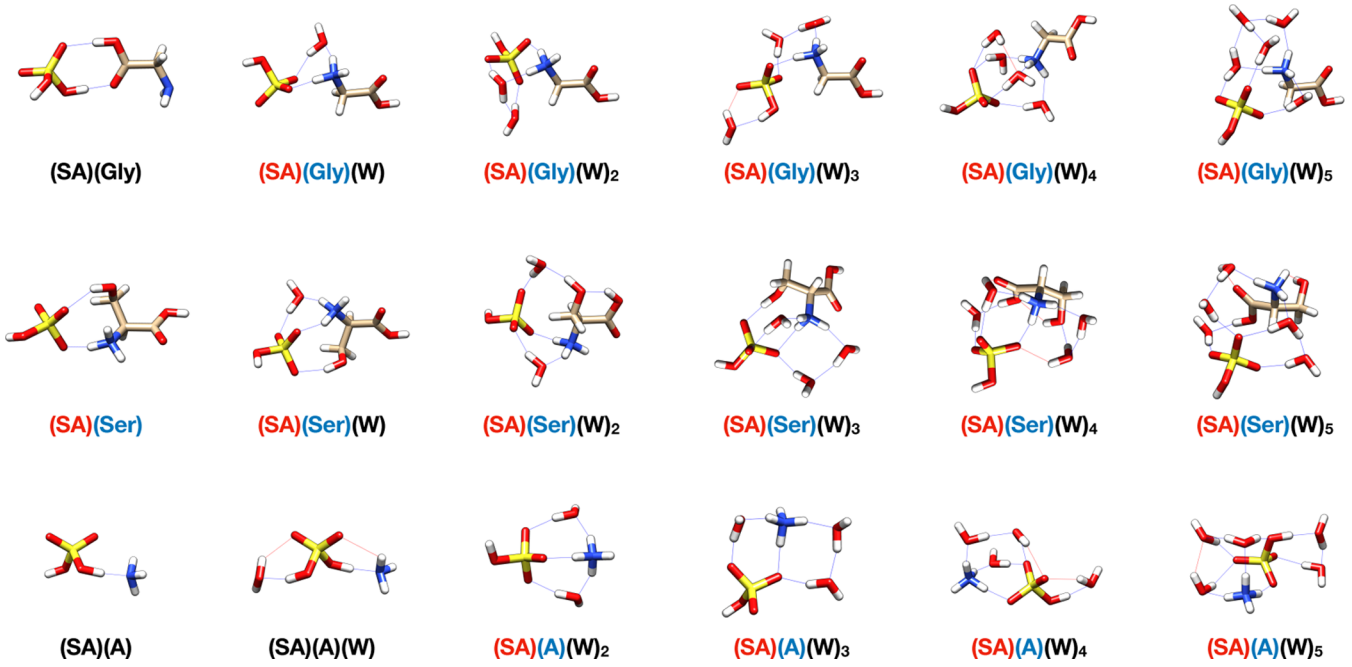

Figure 2. DLPNO-CCSD(T)/CBS//ωb97xD/6-31++G** Gibbs free energy minimum structures of the dry and hydrated sulfuric acid-containing dimers. Hydrogen bonds are indicated with blue lines, close contacts with red lines, and atoms in the colors: H = white, N = blue, O = red, S = yellow, C = beige. Cluster labels are colored such that where there is proton transfer, the protonated molecule label is shown in blue and the deprotonated molecule label is shown in red.

Upon the addition of one water molecule to the sulfuric acid−glycine dimer, the (SA)(Gly)(W) cluster becomes the most stable trimer by about 0.5 kcal mol^{-1} compared to (SA)(Ser)(W). The enthalpy gained by the formation of the hydrogen bond between the Ser methoxy group and SA is not enough to counteract the loss of entropy of the (SA)(Ser)(W) minimum. The hydrogen-bond angle of 159° seems to account for this difference. Furthermore, the proton transfer observed in the (SA)(Gly)(W) accounts for around 2 kcal mol^{-1} in stabilization energy compared to the (SA)(A)(W) cluster, continuing the trend identified in the dry cluster. With the addition of a second water molecule, the stabilizing effect of a proton transfer plays a secondary role as all three systems have undergone proton transfer. Here, the $(SA)(A)(W)_2$ cluster is the most stable by up to 3 kcal mol^{-1} compared to the $(SA)(Gly)(W)_2$ and $(SA)(Ser)(W)_2$ clusters. Ammonia becomes a better nucleator compared to serine and glycine as the ammonium cation is positioned to donate three strong hydrogen bonds, while the protonated Gly and Ser moieties do not.

Previous work by Elm et al. has found slightly different minima for (SA)(Gly)(W) at the M06-2X/6-311++G-

https://doi.org/10.1021/acs.jpca.2c03539
J. Phys. Chem. A 2022, 126, 5195−5206

(3df,3pd) level of theory, where the Gly and SA are held together by two hydrogen bonds and the water is on the other side of the SA (Figure 2 in ref 34). We optimized this structure with the ωb97xD/6-31++G** functional and calculated the DLPNO-CCSD(T)//ωb97xD/6-31++G** ΔG° values at 217 and 298 K and found that this structure has basically the same thermochemistry as our structure in Figure 2, just 0.1 kcal mol^{-1} higher at both temperatures.

The $(SA)(Ser)(W)_{0-3}$ structures have been previously investigated by Ge et al. at the M06-2X/6-311++G(3df,3pd) level.[33] Our structures for $n = 0-2$ are identical to theirs, but their $(SA)(Ser)(W)_3$ free energy minimum is different from ours, where the three water molecules are separated from each other without forming any W−W hydrogen bonds. Examining the Supporting Information (SI), we find that our free energy minimum is identical to their structure "*h*" (Figure S5 in ref 33). We have used our methodology to run all of their $(SA)(Ser)(W)_3$ structures, which are ordered from lowest to highest electronic energy and discovered that their structure "*a*" is the ωb97xD/6-31++G** electronic energy minimum, their structure "*b*" is the DLPNO-CCSD(T)/CBS electronic energy minimum, and their structure "*h*" is the DLPNO-CCSD(T)/CBS//ωb97xD/6-31++G** Gibbs free energy minimum at 217 and 298 K.

Formation of Non-Sulfuric Acid-Containing Dimers. Table 3 lists the Gibbs free energy changes associated with the formation of non-sulfuric acid-containing dimers, with the corresponding geometries shown in Figure 3. Due to large positive Gibbs free energy changes associated with the hydration of the dry dimer, only the dimerization energies are listed, whereas the hydration energies are provided in Table S1 in the Supporting Information. These energies are much more positive than those that contain sulfuric acid (Table 2), supporting the widespread belief that sulfuric acid is the known driver of new particle formation in the atmosphere. Substituting an amino acid for sulfuric acid will not drive new particle formation.[32,33,44]

Table 3. DLPNO-CCSD(T)/CBS//ωb97xD/6-31++G Gibbs Free Energy Changes Associated with the Formation of Glycine−Serine, Glycine−Ammonia, and Serine−Ammonia Dimers at Atmospherically Relevant Temperatures and 1 atm Pressure**

cluster	216.65 K	273.15 K	298.15 K
Gly + Ser ⇌ (Gly)(Ser)	−6.09	−4.01	−3.09
Gly + A ⇌ (Gly)(A)	−3.29	−1.69	−0.98
Ser + A ⇌ (Ser)(A)	−3.70	−2.13	−1.44

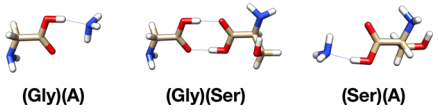

Figure 3. DLPNO-CCSD(T)/CBS//ωb97xD/6-31++G** Gibbs free energy minimum structures of the stable non-sulfuric acid-containing dry dimers. Hydrogen bonds are indicated with blue lines, close contacts with red lines, and atoms in the colors: H = white, N = blue, O = red, S = yellow, C = beige.

Formation and Hydration of Sulfuric Acid-Containing Trimers. Table 4 lists the Gibbs free energy changes associated with the formation of sulfuric acid-containing trimers and their subsequent solvation with up to five water molecules, with the corresponding geometries shown in Figure 4. All three dry trimers, (SA)(Gly)(Ser), (SA)(Gly)(A), and (SA)(Ser)(A), have roughly the same Gibbs free energy of formation, revealing that the amino acids are competitive with ammonia for the formation of prenucleation clusters. As can be viewed in the figure, the (SA)(Gly)(A) structure is the only structure where sulfuric acid does not donate a proton to the base, forming an ionic complex. Our (SA)(Gly)(A) structure is identical to the Elm et al. M06-2X minimum.[34] Upon adding one to three water molecules, sulfuric acid's proton is transferred to Gly, and the fourth and fifth waters result in A being protonated rather than Gly. As Gly (pK_a 9.60) is a slightly better base than A (pK_a 9.25), this is an example of how the subtle interactions between SA, a base, and water molecules change the gas-phase ΔG° minima.

The bottom row of Figure 4 displays the $(SA)(Ser)(A)(W)_{n=0-5}$ ΔG° minima. Ser (pK_a 9.15) is only a slightly weaker base than A, and A is protonated for all species except for $(SA)(Ser)(A)(W)_3$, where Ser is protonated. Once the fifth water is added, Ser becomes a zwitterion and the water network holds the bisulfate anion and the ammonium cation in a tight complex with the zwitterion. This shows how a relatively small water network stabilizes four separate charges, forming a tetra-ionic structure. This results in a stepwise ΔG° value of −5.15 kcal mol^{-1} at 217 K and −2.67 kcal mol^{-1} at 298 K for the addition of the fifth water to the $(SA)(Ser)(A)(W)_4$ cluster.

Contrasting the $(SA)(Gly)(Ser)(W)_{n=0-5}$ minima in the top row of Figure 4, the stronger base Gly is only protonated when no water is present, yet for $n = 1-5$, it is Ser that is protonated in these complexes. This is another example of how hydrogen-bond topology is more important than acid−base strength for understanding the structure and thermodynamics of these gas-phase clusters.[30]

Formation and Hydration of the Tetramer. Table 5 displays the Gibbs free energy changes associated with the formation of the sulfuric acid−glycine−serine−ammonia tetramer and its subsequent solvation with up to five water molecules, with the corresponding geometries shown in Figure 5. For this system, Ser is protonated in the free energy minimum of the dry cluster, which switches to Gly upon adding one water, then switching again to A with the addition of two or three waters. For the $(SA)(Gly)(Ser)(A)(W)_4$ cluster, Ser is the protonated base, and upon addition of the fifth water, A is once again the protonated base. Once again, the subtle interactions between the water network and SA and these three species determines the most stable structures. Gly and Ser have the ability to form hydrogen bonds with their amino and carboxyl ends, and in the case of Ser also with its polar side chain, which results in the free energy minima (Figure 5) for these complexes at the DLPNO/CCSD(T)/CBS//ωb97xD/6-31++G** level of theory.

On the Accuracy of ΔG° Values with Variation of Functionals and Basis Sets. One problem we noted while writing up this paper was that previous ΔG° values reported in the literature for the SA-Gly-A system were much more negative than ours.[32] As the methodologies are similar, we decided to investigate further. Li et al. calculated the ΔG° values using the DLPNO-CCSD(T)/aug-cc-pVTZ electronic energies for M06-2X/6-31++G(d,p) geometries combined with the unscaled M06 Gibbs energy corrections. In Table 6, we present our calculated RRHO DLPNO-CCSD(T)/aug-cc-

https://doi.org/10.1021/acs.jpca.2c03539
J. Phys. Chem. A 2022, 126, 5195−5206

Table 4. DLPNO-CCSD(T)/CBS//ωb97xD/6-31++G** Gibbs Free Energy Changes Associated with the Formation and Sequential Hydration of Sulfuric Acid−Glycine−Serine, Sulfuric Acid−Glycine−Ammonia, and Sulfuric Acid−Serine−Ammonia Trimers at Atmospherically Relevant Temperatures and 1 atm Pressure

cluster	216.65 K	273.15 K	298.15 K
SA + Gly + Ser ⇌ (SA)(Gly)(Ser)	−17.72	−12.97	−10.96
(SA)(Gly)(Ser) + W ⇌ (SA)(Gly)(Ser)(W)	−2.26	−0.90	−0.40
(SA)(Gly)(Ser)(W) + W ⇌ (SA)(Gly)(Ser)$(W)_2$	−8.00	−5.88	−4.77
(SA)(Gly)(Ser)$(W)_2$ + W ⇌ (SA)(Gly)(Ser)$(W)_3$	−0.76	1.26	2.16
(SA)(Gly)(Ser)$(W)_3$ + W ⇌ (SA)(Gly)(Ser)$(W)_4$	−5.57	−3.39	−2.43
(SA)(Gly)(Ser)$(W)_4$ + W ⇌ (SA)(Gly)(Ser)$(W)_5$	5.43	6.90	7.55
SA + Gly + A ⇌ (SA)(Gly)(A)	−17.24	−13.65	−12.07
(SA)(Gly)(A) + W ⇌ (SA)(Gly)(A)(W)	−2.79	−0.94	−0.17
(SA)(Gly)(A)(W) + W ⇌ (SA)(Gly)(A)$(W)_2$	−2.94	−1.10	−0.30
(SA)(Gly)(A)$(W)_2$ + W ⇌ (SA)(Gly)(A)$(W)_3$	−2.10	−0.19	0.71
(SA)(Gly)(A)$(W)_3$ + W ⇌ (SA)(Gly)(A)$(W)_4$	−2.93	−0.63	0.38
(SA)(Gly)(A)$(W)_4$ + W ⇌ (SA)(Gly)(A)$(W)_5$	−1.90	0.37	1.26
SA + Ser + A ⇌ (SA)(Ser)(A)	−17.65	−13.57	−11.78
(SA)(Ser)(A) + W ⇌ (SA)(Ser)(A)(W)	−5.59	−4.13	−3.48
(SA)(Ser)(A)(W) + W ⇌ (SA)(Ser)(A)$(W)_2$	−0.73	1.84	2.99
(SA)(Ser)(A)$(W)_2$ + W ⇌ (SA)(Ser)(A)$(W)_3$	−0.85	0.67	1.21
(SA)(Ser)(A)$(W)_3$ + W ⇌ (SA)(Ser)(A)$(W)_4$	−0.35	1.33	2.19
(SA)(Ser)(A)$(W)_4$ + W ⇌ (SA)(Ser)(A)$(W)_5$	−5.15	−3.43	−2.67

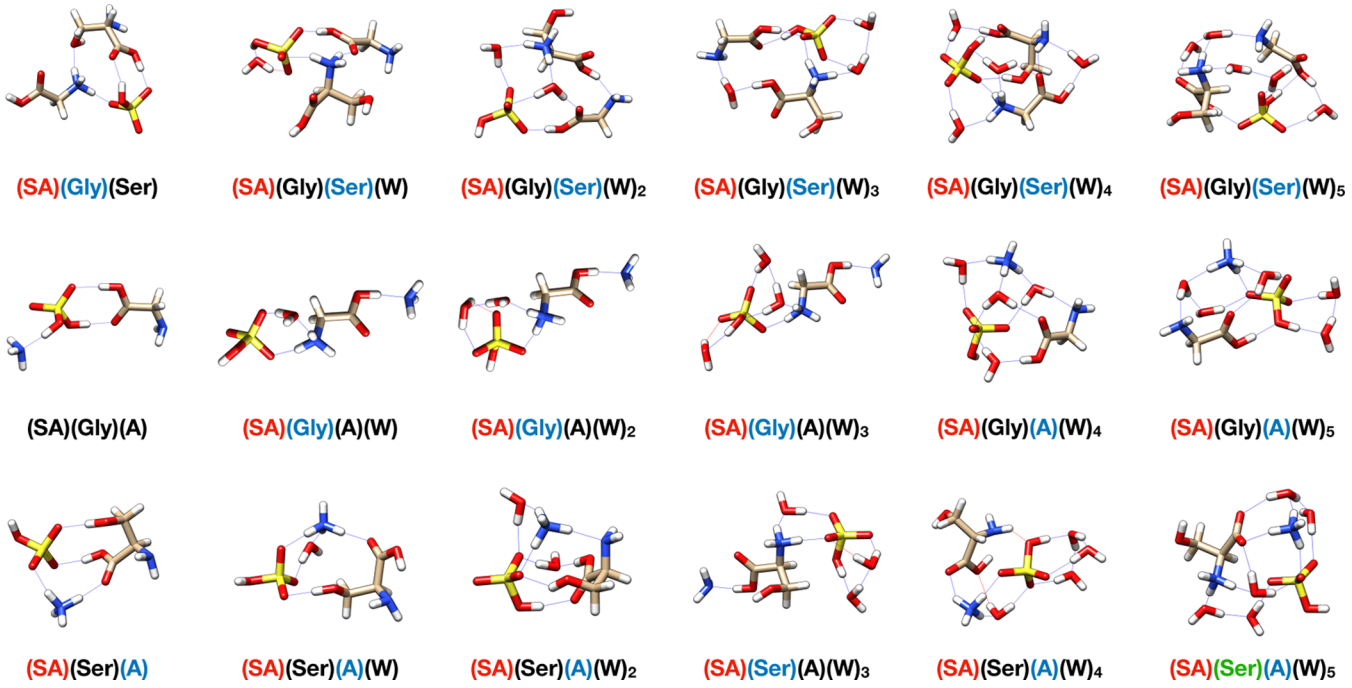

Figure 4. DLPNO-CCSD(T)/CBS//ωb97xD/6-31++G** Gibbs free energy minimum structures of the dry and hydrated sulfuric acid-containing trimers. Hydrogen bonds are indicated with blue lines, close contacts with red lines, and atoms in the colors: H = white, N = blue, O = red, S = yellow, C = beige. Cluster labels are colored such that where there is proton transfer, the protonated molecule label is shown in blue, the deprotonated molecule label in red, and the zwitterion label in green.

pVnZ//DFT ΔG° values for both the ωb97xd/6-31++G** and M06-2X/6-31++G(d,p) geometries, along with the literature values,[32] for the unhydrated SA-Gly-A system. We used ArbAlign to verify that the complexed structures are the same.[108] The RMSD between our M06-2X structures of (SA)(Gly), (SA)(A), (Gly)(A), and (SA)(Gly)(A) and the M06-2X structures reported in the previous paper[32] are 0.018, 0.009, 0.002, and 0.044 Å, respectively. We can learn several important things from this table. First, comparing columns 2 and 3, we see that the two different density functional theory (DFT) functionals do not significantly change the final DLPNO-CCSD(T) values. It does not matter whether one uses ωb97xD or M06-2X for geometry optimization, as the DLPNO-CCSD(T) electronic energies result in ΔG° values that are quite similar, a result that has been reported before for hydrogen-bonded systems.[12,34,42,43,109] Second, we are unable to reproduce the previous results of Li et al.,[32] as their numbers in the last column are much more negative than ours. We note that in their article they used Gaussian 09 for their calculations, while we used Gaussian 16, which is unlikely to be the source of error. It is possible they reported the numbers for their lowest temperature, which was 218 K, rather than the reported

https://doi.org/10.1021/acs.jpca.2c03539
J. Phys. Chem. A 2022, 126, 5195−5206

Table 5. DLPNO-CCSD(T)/CBS//ωb97xD/6-31++G** Gibbs Free Energy Changes Associated with the Formation of Sulfuric Acid−Glycine−Serine−Ammonia Tetramer and Its Subsequent Hydration at Atmospherically Relevant Temperatures and 1 atm Pressure

cluster	216.65 K	273.15 K	298.15 K
SA + Gly + Ser + A ⇌ (SA)(Gly)(Ser)(A)	−22.83	−17.23	−14.77
(SA)(Gly)(Ser)(A) + W ⇌ (SA)(Gly)(Ser)(A)(W)	−3.70	−1.22	−0.12
(SA)(Gly)(Ser)(A)(W) + W ⇌ (SA)(Gly)(Ser)(A)$(W)_2$	−1.47	0.81	1.83
(SA)(Gly)(Ser)(A)$(W)_2$ + W ⇌ (SA)(Gly)(Ser)(A)$(W)_3$	−1.99	0.02	0.91
(SA)(Gly)(Ser)(A)$(W)_3$ + W ⇌ (SA)(Gly)(Ser)(A)$(W)_4$	−3.99	−2.08	−1.24
(SA)(Gly)(Ser)(A)$(W)_4$ + W ⇌ (SA)(Gly)(Ser)(A)$(W)_5$	−0.55	1.55	2.49

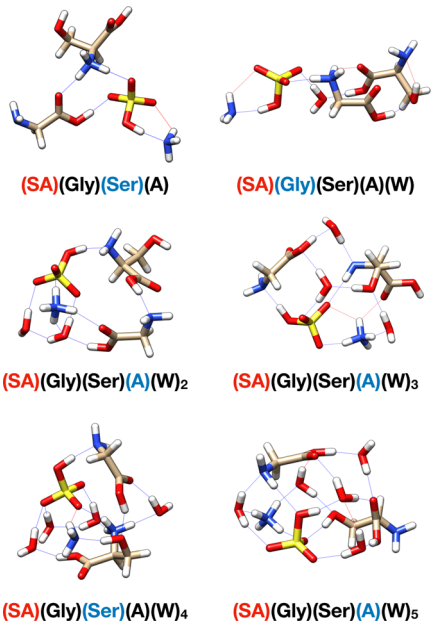

Figure 5. DLPNO-CCSD(T)/CBS//ωb97xD/6-31++G** Gibbs free energy minimum structures of the dry and hydrated sulfuric acid−glycine−serine−ammonia tetramer. Hydrogen bonds are indicated with blue lines, close contacts with red lines, and atoms in the colors: H = white, N = blue, O = red, S = yellow, C = beige. Cluster labels are colored such that where there is proton transfer, the protonated molecule label is shown in blue and the deprotonated molecule label in red.

298 K, by mistake. This would lower the reported energies by about 3 kcal mol^{-1}, as observed for the six dimers reported in Tables 2 and 3.

Table 7 presents the results for the cc-pVnZ (n = D, T, Q) and the aug-cc-pVnZ (n = D,T,Q) basis sets to examine basis set effects for the formation of all of the dry clusters. For each reaction on the left-hand side of the table, the numbers in the top row are for the cc-pVnZ basis set, while the numbers in the second row are for the augmented basis sets where diffuse functions have been added. Augmentation is generally most useful for anions where the electron cloud is bigger, and usually not as important for neutral clusters. We see from the table that the largest differences in the ΔG° values for cluster formation are for the double zeta basis set. The differences narrow for the triple and quadruple basis sets. The CBS extrapolation uses the DZ, TZ, and QZ basis sets, and the table reveals that the difference in the extrapolated CBS values ranges from 0.01 to 0.7 kcal mol^{-1}.

Comparing the CBS scaled values to the individual cc-pVnZ basis sets in Table 7 for the formation of these clusters illustrates a general trend, which is that the CBS extrapolated values using the three basis sets are typically more positive than the individual values, with DZ yielding the most negative ΔG° values, followed by TZ and then QZ.

Atmospheric Concentrations and Implications. The concentration of a particular cluster in the atmosphere can be estimated from the ΔG° values for the stepwise addition of each additional molecule to the previous cluster. The concentration of each larger cluster depends on the concentration of the preceding cluster and the stepwise thermodynamics of cluster formation presented in Tables 2−5. Assuming a closed system, and initial concentration of the monomers, we solve for all of the equilibrium concentrations for the system. Table 8 lists the equilibrium concentrations of all of the possible clusters presented thus far at temperatures corresponding to the bottom of the troposphere (298.15 K) and the top of the troposphere (216.65 K), a standard pressure of 1 atm, and a relative humidity of 100%. This simulation assumes a relative humidity of 100%, which corresponds to water concentrations of 9.9×10^{14} and 7.7×10^{17} at 217 and 298 K, respectively,[1] and starting concentrations of $[SA]_0 = 5 \times 10^7$,[5,6,110] $[Gly]_0$ and $[Ser]_0 = 1 \times 10^8$,[44] and $[A]_0 = 2 \times 10^{11}$ cm^{-3}.[29,111,112] Only those clusters with concentrations greater than 1 cm^{-3} at one of the two temperatures are presented.

Table 8 reveals that assuming we have a closed system consisting of equal initial concentrations of Gly and Ser (10^8 cm^{-3}), NH_3 concentrations that are 3 orders of magnitude higher than the amino acids (10^{11} cm^{-3}), and 100% relative humidity, we would expect detectable concentrations of clusters of Gly with 1−3 waters, clusters of Ser with 1−2 waters, and clusters of NH_3 with 1−3 waters, along with clusters of sulfuric acid with 1−5 waters, at 298 K. Sulfuric acid

Table 6. RRHO DLPNO-CCSD(T)/aug-cc-pVTZ//DFT ΔG° Values in kcal mol^{-1} at 298.15 K for the Formation of Clusters in the Dry SA-Gly-A System for ωb97xD/6-31++G** and M06-2X/6-31++G** DFT Geometries

clustering reaction	ωb97xD/6-31++G**	M06-2X/6-31++G**	M06-2X/6-31++G** ref 32
SA + Gly → (SA)(Gly)	−6.41	−6.60	−9.30
SA + A → (SA)(A)	−6.61	−6.18	−8.34
Gly + A → (Gly)(A)	−1.27	−0.87	−5.58
SA + Gly +A → (SA)(Gly)(A)	−12.92	−12.79	−17.69

https://doi.org/10.1021/acs.jpca.2c03539
J. Phys. Chem. A 2022, 126, 5195−5206

Table 7. DLPNO-CCSD(T) $\Delta G°$ Values in kcal mol^{-1} at 298.15 K for the Formation of Dry Clusters Using the Nonaugmented and Augmented DZ, TZ, and QZ Basis Sets, along with CBS Extrapolation, Using ωb97xD/6-31++G** Geometries and a Scaling Factor of 0.971

cluster reaction	DZ[a]	TZ[b]	QZ[c]	CBS[d]
SA + Gly → (SA)(Gly)	−7.31	−6.21	−5.99	−5.90
	−5.80	−6.51	−6.13	−5.48
SA + Ser → (SA)(Ser)	−7.99	−8.18	−8.66	−9.28
	−10.20	−9.60	−9.25	−8.88
SA + A → (SA)(A)	−8.93	−7.43	−6.88	−6.41
	−6.46	−6.72	−6.60	−6.40
Gly + Ser → (Gly)(Ser)	−5.05	−3.72	−3.35	−3.09
	−3.62	−3.86	−3.52	−3.00
Gly + A → (Gly)(A)	−4.27	−2.31	−1.59	−0.98
	−1.50	−1.38	−1.27	−1.14
Ser + A → (Ser)(A)	−4.83	−2.63	−1.95	−1.44
	−1.96	−1.69	−1.63	−1.58
SA + Gly + Ser → (SA)(Gly)(Ser)	−14.67	−11.96	−11.32	−10.96
	−14.71	−13.27	−11.84	−10.16
SA + Gly + A → (SA)(Gly)(A)	−16.54	−13.65	−12.76	−12.07
	−12.42	−13.13	−12.57	−11.67
SA + Ser + A → (SA)(Ser)(A)	−13.82	−11.18	−11.23	−11.78
	−12.47	−12.22	−11.72	−11.08
Gly + Ser + A → (Gly)(Ser)(A)	−5.90	−2.91	−1.99	−1.30
	−2.83	−2.49	−1.84	−1.00
SA + Gly + Ser + A → (SA)(Gly)(Ser)(A)	−18.69	−15.91	−15.21	−14.77
	−18.55	−17.03	−15.61	−13.96

[a]cc-pVDZ values are listed on top with the aug-cc-pVDZ values below. [b]cc-pVTZ values are listed on top with the aug-cc-pVTZ values below. [c]cc-pVQZ values are listed on top with the aug-cc-pVQZ values below. [d]CBS values are listed on top with the aug-CBS values below.

would form clusters with Gly and 0−3 waters, Ser and 0−4 waters, and NH_3 with 0−4 waters at 217 K. The predicted (Gly)(Ser) concentration is about the same as the (Gly)(A) and (Ser)(A) concentrations at 298 K. The (SA)(Ser)(A)-$(W)_{0-2}$ and (SA)(Gly)(A)$(W)_{0-2}$ predicted concentrations are also quite similar. As can be gleaned from Table 7, Gly and Ser are interchangeable with ammonia because the $\Delta G°$ value for the formation of clusters at 298 K such as (SA)(Ser) is about 3 kcal mol^{-1} more negative than that for (SA)(A) and the corresponding value for the formation of (Gly)(Ser) is 1−1.5 kcal mol^{-1} more negative than for the formation of (Gly)(A) and (Ser)(A). This results from the detailed molecular interactions in the formation of these clusters revealed by the figures. Figure 2 shows that the (SA)(Gly) and (SA)(A) clusters are neutral, while the (SA)(Ser) cluster is di-ionic, with SA losing its proton to serine, leading to a more negative $\Delta G°$. This happens despite serine being a weaker base than glycine or ammonia. The more negative $\Delta G°$ value for the formation of (Gly)(Ser) results from two hydrogen bonds being formed in this cluster, as opposed to only one hydrogen bond being formed for both the (Gly)(A) and (Ser)(A) clusters. This is illustrated in Figure 3. As noted before, the detailed interactions of these clusters are as important as the actual acid/base strength in clusters such as the sulfuric acid−formic acid−ammonia system.[30]

CONCLUSIONS

This computational investigation of the (SA)(Gly)(Ser)(A)-$(W)_{0-5}$ system, where SA = sulfuric acid, Gly = glycine, Ser = serine, A = ammonia, and W = water, reveals how amino acids can compete with ammonia for the formation of complexes containing these molecules. We have partially corrected the harmonic frequencies using a scaling factor and demonstrated that scaling the harmonic frequencies is a better approach than using the quasi-harmonic method. The amino acids glycine and serine are competitive with ammonia in the formation of clusters with sulfuric acid and water because the details of complex formation are more important than base strength. Considering the dimers (SA)(Ser), (SA)(Gly), and (SA)(A), the weakest base, serine, forms the most stable complex, with a $\Delta G°$ for the formation of the (SA)(Ser) complex that is more than 3 kcal mol^{-1} more negative than the other two complexes, a consequence of the strong di-ionic complex formed between the bisulfate ion and the protonated serine cation. For the dimers (Gly)(Ser), (Gly)(A), and (Ser)(A), the (Gly)(Ser) complex is more stable than the other two, as it is the only complex with two hydrogen bonds holding it together, another result stemming from the detailed structure and not related to base strength. For the (SA)(Gly)(Ser)$(W)_n$ complexes, glycine is protonated for the dry complex (n = 0), whereas serine is protonated for all of the wet complexes (n = 1−5). In contrast, for the (SA)(Gly)(A)$(W)_n$ complexes, we predict that the ammonia or the glycine can be protonated depending on the degree of hydration. Either ammonia or serine is protonated for the (SA)(Ser)(A)$(W)_n$ complexes, except for five waters, where the complex contains a zwitterionic serine along with the ammonium cation and the bisulfate anion. The $\Delta G°$ value of the (SA)(Ser)(A)$(W)_5$ complex forming from the four water complex is −5.15 kcal mol^{-1} at 217 K, which is about 5 kcal mol^{-1} more negative than the sequential formation of the four water complex, resulting from the detailed structure of (SA)(Ser)(A)$(W)_5$. In this complex, serine is a zwitterion and the five waters stabilize it along with the bisulfate anion and the ammonium cation. For the largest complex studied, (SA)-(Gly)(Ser)(A)$(W)_n$, serine is protonated for n = 0, 4; ammonia is protonated for n = 2, 3, 5; and glycine is

https://doi.org/10.1021/acs.jpca.2c03539
J. Phys. Chem. A 2022, 126, 5195−5206

Table 8. Equilibrium Concentrations of Sulfuric Acid (SA), Glycine (Gly), Serine (Ser), Ammonia (A), and Water (W) Clusters at Temperatures of 216.65 and 298.15 K Corresponding to the Top and Bottom of the Troposphere[a]

cluster	216.65 K	298.15 K
SA[b]	8.37×10^{5}	2.25×10^{7}
(SA)(W)	7.04×10^{5}	2.28×10^{7}
$(SA)(W)_2$	9.66×10^{4}	4.41×10^{6}
$(SA)(W)_3$	2.12×10^{3}	2.22×10^{5}
$(SA)(W)_4$	9.32×10^{1}	1.81×10^{4}
$(SA)(W)_5$	1.29×10^{-2}	2.77×10^{1}
Gly[c]	9.99×10^{7}	9.95×10^{7}
(Gly)(W)	8.67×10^{4}	5.03×10^{5}
$(Gly)(W)_2$	3.41×10^{2}	7.00×10^{3}
$(Gly)(W)_3$	5.06×10^{-2}	1.74×10^{1}
Ser[d]	8.00×10^{7}	9.88×10^{7}
(Ser)(W)	1.49×10^{5}	1.12×10^{6}
$(Ser)(W)_2$	2.27×10^{1}	1.66×10^{3}
A[e]	2.00×10^{11}	2.00×10^{11}
(A)(W)	6.56×10^{6}	3.79×10^{8}
$(A)(W)_2$	5.60×10^{1}	4.52×10^{4}
$(A)(W)_3$	1.88×10^{-2}	1.03×10^{2}
(SA)(Gly)	1.90×10^{3}	1.92
(SA)(Gly)(W)	9.35×10^{3}	5.27
$(SA)(Gly)(W)_2$	1.04×10^{3}	5.11×10^{-1}
$(SA)(Gly)(W)_3$	4.39	1.20×10^{-2}
(SA)(Ser)	4.61×10^{6}	5.73×10^{2}
(SA)(Ser)(W)	1.30×10^{7}	6.43×10^{2}
$(SA)(Ser)(W)_2$	2.14×10^{6}	1.20×10^{2}
$(SA)(Ser)(W)_3$	1.17×10^{4}	3.83
$(SA)(Ser)(W)_4$	7.66	5.94×10^{-3}
(SA)(A)	2.69×10^{6}	9.12×10^{3}
(SA)(A)(W)	1.88×10^{5}	8.55×10^{2}
$(SA)(A)(W)_2$	2.56×10^{7}	1.96×10^{4}
$(SA)(A)(W)_3$	1.08×10^{4}	9.60×10^{1}
$(SA)(A)(W)_4$	4.34×10^{2}	4.21
(Gly)(Ser)	3.28×10^{2}	7.35×10^{-2}
(Gly)(A)	1.23×10^{3}	4.22
(Ser)(A)	2.55×10^{3}	9.11
(SA)(Gly)(Ser)	4.37	3.95×10^{-8}
$(SA)(Gly)(Ser)(W)_2$	8.36×10^{1}	2.38×10^{-7}
(SA)(Gly)(A)	3.58×10^{3}	5.19×10^{-4}
(SA)(Gly)(A)(W)	6.38×10^{1}	2.16×10^{-5}
$(SA)(Gly)(A)(W)_2$	1.85	1.12×10^{-6}
(SA)(Ser)(A)	7.44×10^{3}	3.16×10^{-4}
(SA)(Ser)(A)(W)	9.47×10^{4}	3.52×10^{-3}
$(SA)(Ser)(A)(W)_2$	1.51×10^{1}	7.08×10^{-7}

[a]Starting concentrations of water were taken as 9.9 × 1014 and 7.7 × 1017 at 216.65 and 298.15 K, respectively. [b]$[H_2SO_4]_0 = 5 \times 10^{7}$. [c]$[Gly]_0 = 1 \times 10^{8}$. [d]$[Ser]_0 = 1 \times 10^{8}$. [e]$[NH_3]_0 = 2 \times 10^{11}$ cm^{-3}.

protonated for $n = 1$. The two amino acids and ammonia are almost interchangeable, and there is no easy way to predict which molecule will be protonated since base strength and chemical intuition are not useful predictors. Comparing diffuse functions for the DLPNO-CCSD(T) corrections to the electronic energy, the results differ significantly for the double zeta basis set. Comparing $\Delta G°$ results for the formation of all of these complexes using the double zeta, triple zeta, and quadruple zeta basis sets, as well as extrapolation to the complete basis set limit, we find that, in general, the $\Delta G°$ values become more positive as the basis set increases in size. By assuming we have a closed system consisting of the two amino acids, sulfuric acid, ammonia, and water and initial starting concentrations of these molecules at two different temperatures spanning the troposphere, we predict that we will have clusters of $(SA)(W)_{n=1-3}$, (Gly)(W), (Ser)(W), (A)(W), $(SA)(Gly)(W)_{n=0-2}$, $(SA)(Ser)(W)_{n=0-3}$, $(SA)(A)(W)_{n=0-3}$, (Gly)(A), (Ser)(A), (SA)(Gly)(A), and $(SA)(Ser)(A)(W)_{n=0-1}$ with concentrations greater than 10^3 cm^{-3} at 217 K. At 298 K, we predict that we will have clusters of $(SA)(W)_{n=1-4}$, $(Gly)(W)_{n=1-2}$, $(Ser)(W)_{n=1-2}$, $(A)(W)_{n=1-2}$, and $(SA)(A)(W)_{n=0,2}$ with concentrations greater than 10^3 cm^{-3}. Prenucleation clusters of 10^2 to 10^3 cm^{-3} are necessary for the formation of aerosols.[1] The predicted atmospheric concentrations are a function of the initial starting concentrations and the $\Delta G°$ values for the formation of each cluster. The most negative $\Delta G°$ values are a function of the detailed molecular interactions of these clusters. These details are more important than the base strength of ammonia, glycine, and serine.

■ ASSOCIATED CONTENT

Supporting Information

The Supporting Information is available free of charge at https://pubs.acs.org/doi/10.1021/acs.jpca.2c03539.

Sequential Hydration (Table S1), derivation of complete basis set limit extrapolation formulas (PDF)

The electronic energies, G correction values, and DLPNO-CCSD(T) electronic energies with the cc-pVnZ basis sets (n = D,T,Q) (XLSX)

The ωB97Xd coordinate files of all structures within one kcal mol^{-1} of the $\Delta G°$ minimum for each system; the .xyz files are organized based on cluster and the number of waters present (ZIP)

■ AUTHOR INFORMATION

Corresponding Author

George C. Shields − *Department of Chemistry, Furman University, Greenville, South Carolina 29613, United States;* orcid.org/0000-0003-1287-8585; Email: george.shields@furman.edu

Authors

Conor J. Bready − *Department of Chemistry, Furman University, Greenville, South Carolina 29613, United States*

Sara Vanovac − *Department of Chemistry, Furman University, Greenville, South Carolina 29613, United States*

Tuguldur T. Odbadrakh − *Department of Chemistry, Furman University, Greenville, South Carolina 29613, United States*

Complete contact information is available at: https://pubs.acs.org/10.1021/acs.jpca.2c03539

Notes

The authors declare no competing financial interest.

■ ACKNOWLEDGMENTS

Funding for this work was provided by grants CHE-1229354, CHE 16626238, CHE-1903871, and CHE-2018427 from the National Science Foundation (G.C.S.), the Arnold and Mabel Beckman Foundation Beckman Scholar Award (C.J.B.), and the Barry M. Goldwater Scholarship (C.J.B.). High-performance computing resources were provided by the Research Corporation for Science Advancement (27446) and the

MERCURY Consortium (www.mercuryconsortium.org).[113,114] Molecular graphics and analyses performed with UCSF Chimera, developed by the Resource for Biocomputing, Visualization, and Informatics at the University of California, San Francisco, with support from NIH P41-GM103311.

REFERENCES

(1) Seinfeld, J. H.; Pandis, S. N. *Atmospheric Chemistry and Physics: From Air Pollution to Climate Change*, 3rd ed.; Wiley, 2016.
(2) Lee, S. H.; Gordon, H.; Yu, H.; Lehtipalo, K.; Haley, R.; Li, Y.; Zhang, R. New Particle Formation in the Atmosphere: From Molecular Clusters to Global Climate. *J. Geophys. Res.: Atmos.* **2019**, *124*, 7098−7146.
(3) Intergovernmental Panel on Climate, C. *Climate Change 2013 − The Physical Science Basis*; Cambridge University Press: Cambridge, United Kingdom and New York, NY, USA, 2014; p 1535.
(4) Sipilä, M.; Berndt, T.; Petäjä, T.; Brus, D.; Vanhanen, J.; Stratmann, F.; Patokoski, J.; Mauldin, R. L.; Hyvärinen, A.-P.; Lihavainen, H.; Kulmala, M. The role of sulfuric acid in atmospheric nucleation. *Science* **2010**, *327*, 1243.
(5) Temelso, B.; Morrell, T. E.; Shields, R. M.; Allodi, M. A.; Wood, E. K.; Kirschner, K. N.; Castonguay, T. C.; Archer, K. A.; Shields, G. C. Quantum mechanical study of sulfuric acid hydration: atmospheric implications. *J. Phys. Chem. A* **2012**, *116*, 2209−2224.
(6) Temelso, B.; Phan, T. N.; Shields, G. C. Computational study of the hydration of sulfuric acid dimers: implications for acid dissociation and aerosol formation. *J. Phys. Chem. A* **2012**, *116*, 9745−9758.
(7) Almeida, J.; Schobesberger, S.; Kurten, A.; Ortega, I. K.; Kupiainen-Maatta, O.; Praplan, A. P.; Adamov, A.; Amorim, A.; Bianchi, F.; Breitenlechner, M.; et al. Molecular understanding of sulphuric acid-amine particle nucleation in the atmosphere. *Nature* **2013**, *502*, 359−363.
(8) Lehtipalo, K.; Rondo, L.; Kontkanen, J.; Schobesberger, S.; Jokinen, T.; Sarnela, N.; Kurten, A.; Ehrhart, S.; Franchin, A.; Nieminen, T.; et al. The effect of acid-base clustering and ions on the growth of atmospheric nano-particles. *Nat. Commun.* **2016**, *7*, No. 11594.
(9) Nadykto, A. B.; Yu, F. Strong hydrogen bonding between atmospheric nucleation precursors and common organics. *Chem. Phys. Lett.* **2007**, *435*, 14−18.
(10) Zhang, R.; Jiang, S.; Liu, Y.-R.; Wen, H.; Feng, Y.-J.; Huang, T.; Huang, W. An investigation about the structures, thermodynamics and kinetics of the formic acid involved molecular clusters. *Chem. Phys.* **2018**, *507*, 44−50.
(11) Kerminen, V.-M.; Chen, X.; Vakkari, V.; Petäjä, T.; Kulmala, M.; Bianchi, F. Atmospheric new particle formation and growth: review of field observations. *Environ. Res. Lett.* **2018**, *13*, No. 103003.
(12) Elm, J.; Kubečka, J.; Besel, V.; Jääskeläinen, M. J.; Halonen, R.; Kurtén, T.; Vehkamäki, H. Modeling the formation and growth of atmospheric molecular clusters: A review. *J. Aerosol Sci.* **2020**, *149*, No. 105621.
(13) Leonardi, A.; Ricker, H. M.; Gale, A. G.; Ball, B. T.; Odbadrakh, T. T.; Shields, G. C.; Navea, J. G. Particle formation and surface processes on atmospheric aerosols: A review of applied quantum chemical calculations. *Int. J. Quantum Chem.* **2020**, *120*, No. e26350.
(14) Smith, J. N.; Draper, D. C.; Chee, S.; Dam, M.; Glicker, H.; Myers, D.; Thomas, A. E.; Lawler, M. J.; Myllys, N. Atmospheric clusters to nanoparticles: Recent progress and challenges in closing the gap in chemical composition. *J. Aerosol Sci.* **2021**, *153*, No. 105733.
(15) Loukonen, V.; Kurtén, T.; Ortega, I. K.; Vehkamäki, H.; Pádua, A. A. H.; Sellegri, K.; Kulmala, M. Enhancing effect of dimethylamine in sulfuric acid nucleation in the presence of water − a computational study. *Atmos. Chem. Phys.* **2010**, *10*, 4961−4974.
(16) Leverentz, H. R.; Siepmann, J. I.; Truhlar, D. G.; Loukonen, V.; Vehkamaki, H. Energetics of atmospherically implicated clusters made of sulfuric acid, ammonia, and dimethyl amine. *J. Phys. Chem. A* **2013**, *117*, 3819−3825.
(17) Bustos, D. J.; Temelso, B.; Shields, G. C. Hydration of the sulfuric acid-methylamine complex and implications for aerosol formation. *J. Phys. Chem. A* **2014**, *118*, 7430−7441.
(18) Jen, C. N.; McMurry, P. H.; Hanson, D. R. Stabilization of sulfuric acid dimers by ammonia, methylamine, dimethylamine, and trimethylamine. *J. Geophys. Res.: Atmos.* **2014**, *119*, 7502−7514.
(19) Nadykto, A. B.; Herb, J.; Yu, F.; Xu, Y. Enhancement in the production of nucleating clusters due to dimethylamine and large uncertainties in the thermochemistry of amine-enhanced nucleation. *Chem. Phys. Lett.* **2014**, *609*, 42−49.
(20) Elm, J.; Jen, C. N.; Kurtén, T.; Vehkamäki, H. Strong hydrogen bonded molecular interactions between atmospheric diamines and sulfuric acid. *J. Phys. Chem. A* **2016**, *120*, 3693−3700.
(21) Myllys, N.; Elm, J.; Halonen, R.; Kurten, T.; Vehkamaki, H. Coupled Cluster Evaluation of the Stability of Atmospheric Acid-Base Clusters with up to 10 Molecules. *J. Phys. Chem. A* **2016**, *120*, 621−630.
(22) Elm, J. Elucidating the Limiting Steps in Sulfuric Acid-Base New Particle Formation. *J. Phys. Chem. A* **2017**, *121*, 8288−8295.
(23) Chee, S.; Barsanti, K.; Smith, J. N.; Myllys, N. A predictive model for salt nanoparticle formation using heterodimer stability calculations. *Atmos. Chem. Phys.* **2021**, *21*, 11637−11654.
(24) Xie, H.-B.; Elm, J. Tri-Base Synergy in Sulfuric Acid-Base Clusters. *Atmosphere* **2021**, *12*, 1260.
(25) Han, J.; Wang, L.; Zhang, H.; Su, Q.; Zhou, X.; Liu, S. Determinant Factor for Thermodynamic Stability of Sulfuric Acid-Amine Complexes. *J. Phys. Chem. A* **2020**, *124*, 10246−10257.
(26) Myllys, N.; Kubečka, J.; Besel, V.; Alfaouri, D.; Olenius, T.; Smith, J. N.; Passananti, M. Role of base strength, cluster structure and charge in sulfuric-acid-driven particle formation. *Atmos. Chem. Phys.* **2019**, *19*, 9753−9768.
(27) Waller, S. E.; Yang, Y.; Castracane, E.; Racow, E. E.; Kreinbihl, J. J.; Nickson, K. A.; Johnson, C. J. The Interplay Between Hydrogen Bonding and Coulombic Forces in Determining the Structure of Sulfuric Acid-Amine Clusters. *J. Phys. Chem. Lett.* **2018**, *9*, 1216−1222.
(28) Yang, Y.; Waller, S. E.; Kreinbihl, J. J.; Johnson, C. J. Direct Link between Structure and Hydration in Ammonium and Aminium Bisulfate Clusters Implicated in Atmospheric New Particle Formation. *J. Phys. Chem. Lett.* **2018**, *9*, 5647−5652.
(29) Temelso, B.; Morrison, E. F.; Speer, D. L.; Cao, B. C.; Appiah-Padi, N.; Kim, G.; Shields, G. C. Effect of Mixing Ammonia and Alkylamines on Sulfate Aerosol Formation. *J. Phys. Chem. A* **2018**, *122*, 1612−1622.
(30) Harold, S. E.; Bready, C. J.; Juechter, L. A.; Kurfman, L. A.; Vanovac, S.; Fowler, V. R.; Mazaleski, G. E.; Odbadrakh, T. T.; Shields, G. C. Hydrogen-Bond Topology Is More Important Than Acid/Base Strength in Atmospheric Prenucleation Clusters. *J. Phys. Chem. A* **2022**, *126*, 1718−1728.
(31) Yang, Y.; Johnson, C. J. Hydration motifs of ammonium bisulfate clusters of relevance to atmospheric new particle formation. *Faraday Discuss.* **2019**, *217*, 47−66.
(32) Li, D.; Chen, D.; Liu, F.; Wang, W. Role of glycine on sulfuric acid-ammonia clusters formation: Transporter or participator. *J. Environ. Sci.* **2020**, *89*, 125−135.
(33) Ge, P.; Luo, G.; Luo, Y.; Huang, W.; Xie, H.; Chen, J.; Qu, J. Molecular understanding of the interaction of amino acids with sulfuric acid in the presence of water and the atmospheric implication. *Chemosphere* **2018**, *210*, 215−223.
(34) Elm, J.; Fard, M.; Bilde, M.; Mikkelsen, K. V. Interaction of glycine with common atmospheric nucleation precursors. *J. Phys. Chem. A* **2013**, *117*, 12990−12997.
(35) Wang, C. Y.; Ma, Y.; Chen, J.; Jiang, S.; Liu, Y. R.; Wen, H.; Feng, Y. J.; Hong, Y.; Huang, T.; Huang, W. Bidirectional Interaction of Alanine with Sulfuric Acid in the Presence of Water and the Atmospheric Implication. *J. Phys. Chem. A* **2016**, *120*, 2357−2371.
(36) Hou, G.-L.; Lin, W.; Wang, X.-B. Direct Observation of Hierarchic Molecular Interactions Critical to Biogenic Aerosol Formation. *Commun. Chem.* **2018**, *1*, No. 37.

https://doi.org/10.1021/acs.jpca.2c03539
J. Phys. Chem. A 2022, 126, 5195−5206

(37) Myllys, N.; Myers, D.; Chee, S.; Smith, J. N. Molecular properties affecting the hydration of acid-base clusters. *Phys. Chem. Chem. Phys.* **2021**, *23*, 13106−13114.
(38) Triesch, N.; van Pinxteren, M.; Salter, M.; Stolle, C.; Pereira, R.; Zieger, P.; Herrmann, H. Sea Spray Aerosol Chamber Study on Selective Transfer and Enrichment of Free and Combined Amino Acids. *ACS Earth Space Chem.* **2021**, *5*, 1564−1574.
(39) Angle, K. J.; Nowak, C. M.; Davasam, A.; Dommer, A. C.; Wauer, N. A.; Amaro, R. E.; Grassian, V. H. Amino Acids Are Driven to the Interface by Salts and Acidic Environments. *J. Phys. Chem. Lett.* **2022**, *13*, 2824−2829.
(40) Danger, G.; Plasson, R.; Pascal, R. Pathways for the formation and evolution of peptides in prebiotic environments. *Chem. Soc. Rev.* **2012**, *41*, 5416−5429.
(41) Griffith, E. C.; Vaida, V. In situ observation of peptide bond formation at the water-air interface. *Proc. Natl. Acad. Sci. U.S.A.* **2012**, *109*, 15697−15701.
(42) Gale, A. G.; Odbadrakh, T. T.; Ball, B. T.; Shields, G. C. Water-Mediated Peptide Bond Formation in the Gas Phase: A Model Prebiotic Reaction. *J. Phys. Chem. A* **2020**, *124*, 4150−4159.
(43) Gale, A. G.; Odbadrakh, T. T.; Shields, G. C. Catalytic activity of water molecules in gas-phase glycine dimerization. *Int. J. Quantum Chem.* **2020**, *120*, No. e26469.
(44) Ball, B. T.; Vanovac, S.; Odbadrakh, T. T.; Shields, G. C. Monomers of Glycine and Serine Have a Limited Ability to Hydrate in the Atmosphere. *J. Phys. Chem. A* **2021**, *125*, 8454−8467.
(45) Odbadrakh, T. T.; Gale, A. G.; Ball, B. T.; Temelso, B.; Shields, G. C. Computation of Atmospheric Concentrations of Molecular Clusters from ab initio Thermochemistry. *J. Visualized Exp.* **2020**, *158*, No. e60964.
(46) Kurfman, L. A.; Odbadrakh, T. T.; Shields, G. C. Calculating Reliable Gibbs Free Energies for Formation of Gas-Phase Clusters that Are Critical for Atmospheric Chemistry: (H2SO4)3. *J. Phys. Chem. A* **2021**, *125*, 3169−3176.
(47) Pracht, P.; Bohle, F.; Grimme, S. Automated exploration of the low-energy chemical space with fast quantum chemical methods. *Phys. Chem. Chem. Phys.* **2020**, *22*, 7169−7192.
(48) Grimme, S.; Bannwarth, C.; Shushkov, P. A Robust and Accurate Tight-Binding Quantum Chemical Method for Structures, Vibrational Frequencies, and Noncovalent Interactions of Large Molecular Systems Parametrized for All spd-Block Elements (Z = 1-86). *J. Chem. Theory Comput.* **2017**, *13*, 1989−2009.
(49) Grimme, S. Exploration of Chemical Compound, Conformer, and Reaction Space with Meta-Dynamics Simulations Based on Tight-Binding Quantum Chemical Calculations. *J. Chem. Theory Comput.* **2019**, *15*, 2847−2862.
(50) Bannwarth, C.; Ehlert, S.; Grimme, S. GFN2-xTB-An Accurate and Broadly Parametrized Self-Consistent Tight-Binding Quantum Chemical Method with Multipole Electrostatics and Density-Dependent Dispersion Contributions. *J. Chem. Theory Comput.* **2019**, *15*, 1652−1671.
(51) Elm, J. Clusteromics I: Principles, Protocols, and Applications to Sulfuric Acid-Base Cluster Formation. *ACS Omega* **2021**, *6*, 7804−7814.
(52) Hostaš, J.; Řezáč, J.; Hobza, P. On the performance of the semiempirical quantum mechanical PM6 and PM7 methods for noncovalent interactions. *Chem. Phys. Lett.* **2013**, *568-569*, 161−166.
(53) Stewart, J. J. P. An investigation into the applicability of the semiempirical method PM7 for modeling the catalytic mechanism in the enzyme chymotrypsin. *J. Mol. Model.* **2017**, *23*, 154.
(54) Dieterich, J. M.; Hartke, B. OGOLEM: Global cluster structure optimisation for arbitrary mixtures of flexible molecules. A multi-scaling, object-oriented approach. *Mol. Phys.* **2010**, *108*, 279−291.
(55) Dieterich, J. M.; Hartke, B. Empirical review of standard benchmark functions using evolutionary global optimization. *Appl. Math.* **2012**, *03*, 1552−1564.
(56) Chai, J. D.; Head-Gordon, M. Long-range corrected hybrid density functionals with damped atom-atom dispersion corrections. *Phys. Chem. Chem. Phys.* **2008**, *10*, 6615−6620.
(57) Chai, J. D.; Head-Gordon, M. Systematic optimization of long-range corrected hybrid density functionals. *J. Chem. Phys.* **2008**, *128*, No. 084106.
(58) Ditchfield, R.; Hehre, W. J.; Pople, J. A. Self-Consistent Molecular-Orbital Methods. IX. An Extended Gaussian-Type Basis for Molecular-Orbital Studies of Organic Molecules. *J. Chem. Phys.* **1971**, *54*, 724−728.
(59) Hehre, W. J.; Ditchfield, R.; Pople, J. A. Self—Consistent Molecular Orbital Methods. XII. Further Extensions of Gaussian—Type Basis Sets for Use in Molecular Orbital Studies of Organic Molecules. *J. Chem. Phys.* **1972**, *56*, 2257−2261.
(60) Hariharan, P. C.; Pople, J. A. The influence of polarization functions on molecular orbital hydrogenation energies. *Theor. Chim. Acta* **1973**, *28*, 213−222.
(61) Francl, M. M.; Pietro, W. J.; Hehre, W. J.; Binkley, J. S.; Gordon, M. S.; DeFrees, D. J.; Pople, J. A. Self-consistent molecular orbital methods. XXIII. A polarization-type basis set for second-row elements. *J. Chem. Phys.* **1982**, *77*, 3654−3665.
(62) Frisch, M. J.; Pople, J. A.; Binkley, J. S. Self-consistent molecular orbital methods 25. Supplementary functions for Gaussian basis sets. *J. Chem. Phys.* **1984**, *80*, 3265−3269.
(63) Frisch, M. J.; Trucks, G. W.; Schlegel, H. B.; Scuseria, G. E.; Robb, M. A.; Cheeseman, J. R.; Scalmani, G.; Barone, V.; Petersson, G. A.; Nakatsuji, H.et al. *Gaussian 16 Rev. B.01*; Wallingford, CT 2016.
(64) Neese, F.; Hansen, A.; Liakos, D. G. Efficient and accurate approximations to the local coupled cluster singles doubles method using a truncated pair natural orbital basis. *J. Chem. Phys.* **2009**, *131*, No. 064103.
(65) Neese, F.; Wennmohs, F.; Hansen, A. Efficient and accurate local approximations to coupled-electron pair approaches: An attempt to revive the pair natural orbital method. *J. Chem. Phys.* **2009**, *130*, No. 114108.
(66) Riplinger, C.; Neese, F. An efficient and near linear scaling pair natural orbital based local coupled cluster method. *J. Chem. Phys.* **2013**, *138*, No. 034106.
(67) Riplinger, C.; Sandhoefer, B.; Hansen, A.; Neese, F. Natural triple excitations in local coupled cluster calculations with pair natural orbitals. *J. Chem. Phys.* **2013**, *139*, No. 134101.
(68) Liakos, D. G.; Neese, F. Is it possible to obtain coupled cluster quality energies at near density functional theory cost? Domain-based local pair natural orbital coupled cluster vs modern density functional theory. *J. Chem. Theory Comput.* **2015**, *11*, 4054−4063.
(69) Liakos, D. G.; Sparta, M.; Kesharwani, M. K.; Martin, J. M.; Neese, F. Exploring the Accuracy Limits of Local Pair Natural Orbital Coupled-Cluster Theory. *J. Chem. Theory Comput.* **2015**, *11*, 1525−1539.
(70) Riplinger, C.; Pinski, P.; Becker, U.; Valeev, E. F.; Neese, F. SparseMaps - A systematic infrastructure for reduced-scaling electronic structure methods. II. Linear scaling domain based pair natural orbital coupled cluster theory. *J. Chem. Phys.* **2016**, *144*, No. 024109.
(71) Pavošević, F.; Peng, C.; Pinski, P.; Riplinger, C.; Neese, F.; Valeev, E. F. SparseMaps-A systematic infrastructure for reduced scaling electronic structure methods. V. Linear scaling explicitly correlated coupled-cluster method with pair natural orbitals. *J. Chem. Phys.* **2017**, *146*, No. 174108.
(72) Guo, Y.; Riplinger, C.; Becker, U.; Liakos, D. G.; Minenkov, Y.; Cavallo, L.; Neese, F. Communication: An improved linear scaling perturbative triples correction for the domain based local pair-natural orbital based singles and doubles coupled cluster method [DLPNO-CCSD(T)]. *J. Chem. Phys.* **2018**, *148*, No. 011101.
(73) Liakos, D. G.; Guo, Y.; Neese, F. Comprehensive Benchmark Results for the Domain Based Local Pair Natural Orbital Coupled Cluster Method (DLPNO-CCSD(T)) for Closed- and Open-Shell Systems. *J. Phys. Chem. A* **2020**, *124*, 90−100.
(74) Dunning, T. H. Gaussian basis sets for use in correlated molecular calculations. I. The atoms boron through neon and hydrogen. *J. Chem. Phys.* **1989**, *90*, 1007−1023.

https://doi.org/10.1021/acs.jpca.2c03539
J. Phys. Chem. A 2022, 126, 5195−5206

(75) Kendall, R. A.; Dunning, T. H.; Harrison, R. J. Electron affinities of the first-row atoms revisited. Systematic basis sets and wave functions. *J. Chem. Phys.* **1992**, *96*, 6796−6806.
(76) Wilson, A. K.; van Mourik, T.; Dunning, T. H. Gaussian basis sets for use in correlated molecular calculations. VI. Sextuple zeta correlation consistent basis sets for boron through neon. *J. Mol. Struct.: THEOCHEM* **1996**, *388*, 339−349.
(77) Neese, F. The ORCA program system. *Wiley Interdiscip. Rev.: Comput. Mol. Sci.* **2012**, *2*, 73−78.
(78) Neese, F.; Wennmohs, F.; Becker, U.; Riplinger, C. The ORCA quantum chemistry program package. *J. Chem. Phys.* **2020**, *152*, No. 224108.
(79) Helgaker, T.; Klopper, W.; Koch, H.; Noga, J. Basis-set convergence of correlated calculations on water. *J. Chem. Phys.* **1997**, *106*, 9639−9646.
(80) Irikura, K. K. *THERMO.PL*, NIST, 2002.
(81) Pitzer, K. S.; Gwinn, W. D. Energy levels and thermodynamic functions for molecules with internal rotation I. Rigid frame with attached tops. *J. Chem. Phys.* **1942**, *10*, 428−440.
(82) Isayev, O.; Gorb, L.; Leszczynski, J. Theoretical calculations: Can Gibbs free energy for intermolecular complexes be predicted efficiently and accurately? *J. Comput. Chem.* **2007**, *28*, 1598−1609.
(83) Temelso, B.; Shields, G. C. The Role of Anharmonicity in Hydrogen-Bonded Systems: The Case of Water Clusters. *J. Chem. Theory Comput.* **2011**, *7*, 2804−2817.
(84) Barone, V. Vibrational zero-point energies and thermodynamic functions beyond the harmonic approximation. *J. Chem. Phys.* **2004**, *120*, 3059−3065.
(85) Barone, V. Anharmonic vibrational properties by a fully automated second-order perturbative approach. *J. Chem. Phys.* **2005**, *122*, 14108.
(86) Kjaergaard, H. G.; Garden, A. L.; Chaban, G. M.; Gerber, R. B.; Matthews, D. A.; Stanton, J. F. Calculation of vibrational transition frequencies and intensities in water dimer: Comparison of different vibrational approaches. *J. Phys. Chem. A* **2008**, *112*, 4324−4335.
(87) Diri, K.; Myshakin, E. M.; Jordan, K. D. On the contribution of vibrational anharmonicity to the binding energies of water clusters. *J. Phys. Chem. A* **2005**, *109*, 4005−4009.
(88) Dunn, M. E.; Evans, T. M.; Kirschner, K. N.; Shields, G. C. Prediction of accurate anharmonic experimental vibrational frequencies for water clusters, (H2O)n, n = 2-5. *J. Phys. Chem. A* **2006**, *110*, 303−309.
(89) Njegic, B.; Gordon, M. S. Exploring the effect of anharmonicity of molecular vibrations on thermodynamic properties. *J. Chem. Phys.* **2006**, *125*, No. 224102.
(90) Bégué, D.; Baraille, I.; Garrain, P.; Dargelos, A.; Tassaing, T. Calculation of IR frequencies and intensities in electrical and mechanical anharmonicity approximations: Application to small water clusters. *J. Chem. Phys.* **2010**, *133*, No. 034102.
(91) Dykstra, C. E.; Shuler, K.; Young, R. A.; Bačić, Z. Anharmonicity effects on zero point energies of weakly bound molecular clusters. *J. Mol. Struct.: THEOCHEM* **2002**, *591*, 11−18.
(92) Day, M. B.; Kirschner, K. N.; Shields, G. C. Global search for minimum energy (H2O)n clusters, n = 3-5. *J. Phys. Chem. A* **2005**, *109*, 6773−6778.
(93) Temelso, B.; Archer, K. A.; Shields, G. C. Benchmark structures and binding energies of small water clusters with anharmonicity corrections. *J. Phys. Chem. A* **2011**, *115*, 12034−12046.
(94) Dunn, M. E.; Pokon, E. K.; Shields, G. C. Thermodynamics of forming water clusters at various temperatures and pressures by Gaussian-2, Gaussian-3, Complete Basis Set-QB3, and Complete Basis Set-APNO model chemistries; Implications for atmospheric chemistry. *J. Am. Chem. Soc.* **2004**, *126*, 2647−2653.
(95) Morrell, T. E.; Shields, G. C. Atmospheric implications for formation of clusters of ammonium and 1-10 water molecules. *J. Phys. Chem. A* **2010**, *114*, 4266−4271.
(96) Torrent-Sucarrat, M.; Anglada, J. M.; Luis, J. Role of vibrational anharmonicity in atmospheric radical hydrogen-bonded complexes. *Phys. Chem. Chem. Phys.* **2009**, *11*, 6377−6388.
(97) Kurten, T.; Noppel, M.; Vehkamaki, H.; Salonen, M.; Kulmala, M. Quantum chemical studies of hydrate formation of H_2SO_4 and HSO_4^-. *Boreal Environ. Res.* **2007**, *12*, 431−453.
(98) Hanson, D. R.; Eisele, F. Diffusion of H2SO4 in Humidified Nitrogen: Hydrated H2SO4. *J. Phys. Chem. A* **2000**, *104*, 1715−1719.
(99) Irikura, K. K. Prediction and estimation of molecular thermodynamics. In *Computational Thermochemistry*, Irikura, K. K.; Frurip, D. J., Eds.; American Chemical Society, 1998.
(100) Mammen, M.; Shakhnovich, E. I.; Deutch, J. M.; Whitesides, G. M. Estimating the Entropic Cost of Self-Assembly of Multiparticle Hydrogen-Bonded Aggregates Based on the Cyanuric Acid·Melamine Lattice. *J. Org. Chem.* **1998**, *63*, 3821−3830.
(101) Alecu, I. M.; Zheng, J.; Zhao, Y.; Truhlar, D. G. Computational Thermochemistry: Scale Factor Databases and Scale Factors for Vibrational Frequencies Obtained from Electronic Model Chemistries. *J. Chem. Theory Comput.* **2010**, *6*, 2872−2887.
(102) Grimme, S. Supramolecular binding thermodynamics by dispersion-corrected density functional theory. *Chem. − Eur. J.* **2012**, *18*, 9955−9964.
(103) Kanchanakungwankul, S.; Bao, J. L.; Zheng, J.; Alecu, I. M.; Lynch, B. J.; Truhlar, D. G. Database of frequency scale factors for electronic model chemistries - Version 5. 2021.
(104) Bowman, J. M. Self-consistent field energies and wavefunctions for coupled oscillatros. *J. Chem. Phys.* **1978**, *68*, 608.
(105) Gerber, R. B.; Ratner, M. A. A semiclassical self-consistent field (SC-SCF) approximation for eigenvalues of coupled-vibration systems. *Chem. Phys. Lett.* **1979**, *68*, 195−198.
(106) Matsunaga, N.; Chaban, G. M.; Gerber, R. B. Degenerate perturbation theory corrections for the vibrational self-consistent field approximation: Method and applications. *J. Chem. Phys.* **2002**, *117*, 3541.
(107) Neff, M.; Rauhut, G. Toward large scale vibrational configuration interaction calculations. *J. Chem. Phys.* **2009**, *131*, No. 124129.
(108) Temelso, B.; Mabey, J. M.; Kubota, T.; Appiah-Padi, N.; Shields, G. C. ArbAlign: A Tool for Optimal Alignment of Arbitrarily Ordered Isomers Using the Kuhn-Munkres Algorithm. *J. Chem. Inf. Model.* **2017**, *57*, 1045−1054.
(109) Elm, J.; Bilde, M.; Mikkelsen, K. V. Assessment of binding energies of atmospherically relevant clusters. *Phys. Chem. Chem. Phys.* **2013**, *15*, 16442−16445.
(110) Curtius, J.; Lovejoy, E. R.; Froyd, K. D. Atmospheric Ion-induced Aerosol Nucleation. *Space Sci. Rev.* **2007**, *125*, 159−167.
(111) Ge, X.; Wexler, A. S.; Clegg, S. L. Atmospheric amines - Part I. A review. *Atmos. Environ.* **2011**, *45*, 524−546.
(112) Ge, X.; Wexler, A. S.; Clegg, S. L. Atmospheric amines - Part II. Thermodynamic properties and gas/particle partitioning. *Atmos. Environ.* **2011**, *45*, 561−577.
(113) Shields, G. C. Twenty years of exceptional success: The molecular education and research consortium in undergraduate computational chemistry (MERCURY). *Int. J. Quantum Chem.* **2020**, *120*, No. e26274.
(114) Shields, G. C. The Molecular Education and Research Consortium in Undergraduate computational chemistRY (MERCURY): Twenty years of exceptional success supporting undergraduate research and inclusive excellence. *Scholarship Pract. Undergrad. Res.* **2020**, *3*, 5−15.

https://doi.org/10.1021/acs.jpca.2c03539
J. Phys. Chem. A 2022, 126, 5195−5206